

Confronting Einstein Yang Mills Higgs Dark Energy in light of observations

Debabrata Adak

Department of Physics, Government General Degree College Singur, Jalaghata
Hooghly-712409, West Bengal, India

debabrata.adak.sinp@gmail.com

Abstract

We study the observational aspects of Einstein Yang Mills Higgs Dark energy model and constrain the parameter space from the latest observational data from type Ia supernovae, observational Hubble data, baryon acoustic oscillation data and cosmic microwave background radiation shift parameter data. It is found from the analysis of data that the Higgs field in presence of gauge fields can successfully describe the present accelerated expansion of the universe consistent with the astrophysical observations.

1 Introduction

Cosmic acceleration discovered more than two decades ago by supernova projects [1, 2] is perhaps the most important and fascinating phenomenon that still remains in mystery. This cosmic acceleration can be accounted for by invoking the presence of some exotic fluid dubbed dark energy with negative pressure to overcome the gravitational collapse and thereby resulting in the accelerated expansion of the universe [3–6]. From the observations it is evident that it constitute about 68% of the total energy density in the universe [7]. The cosmological constant Λ is the best fitted model so far to explain this recent accelerated expansion of the universe. However it suffers from two major theoretical problems known as fine tuning problem [8] and cosmic coincidence problem [9]. Despite being consistent with the observations, these problems of cosmological constant make the cosmologists search for alternatives.

A simplest alternative is the canonical scalar field model known as “quintessence” [9]. The potential of the canonical scalar field is so chosen that the field rolls very slowly at the present epoch resulting in the negative pressure of the field which leads to cosmic acceleration. This essentially requires the potential to be very flat with respect to the field ϕ resulting in the mass of the field around 10^{-33} eV. The tracker behaviour of the scalar field model [10] helps to alleviate the problem of cosmic coincidence in the dark energy scenario. Explaining the late time cosmic acceleration is also possible from the modification of gravity at the large scales known as infrared modification of gravity. It is found that higher order curvature invariants play an important role in modification of gravity at large scales thereby leading to accelerated expansion of the universe at the present epoch [11–13]. Moreover higher dimensional models of gravity induces modification of Einstein’s gravity in the 3+1 dimensional effective theory at large scales leading to the accelerated expansion of the universe [14, 15]. A large number of modified gravity models is tested to be free from ghost or tachyon instabilities and they also do not conflict with the solar system constraints (see [16] and references therein for a review on cosmology driven by modified gravity models). Of late the detections of GW170817 and GRB 170817A revealed the fact that the speed of gravitational waves differs from the speed

of light by one part in 10^{15} [17–21]. This discovery have severely constrained these modified gravity models as well as other dark energy models [22–28].

From the standard model of particle physics this is well known that all the particle in the universe gets mass due to their interaction with the Higgs field [29, 30]. The dynamics of FRW universe was studied in presence of non-abelian gauge fields invariant under $\text{SO}(3)$ and $\text{SU}(2)$ gauge group or an arbitrary gauge group $\text{SO}(N)$ [31–33]. In the context of inflation Einstein Yang-Mills Higgs action was first introduced [34, 35] to study the effect of gauge field on inflation. Recently in [36], the dynamics of this non-abelian Higgs field coupled to gravity was studied in the context of late time cosmic acceleration. In the work [37], considering the interaction in $\text{SU}(2)$ representation for Higgs field the authors have studied the dynamics of cosmology in Einstein Yang-Mills Higgs to explain the recent accelerated expansion of the Universe. What is not yet known is that the viability of this model in respect of cosmological observations.

In the present work we study the viability of the Einstein Yang-Mills Higgs dark energy in the context of observational data. We constrain the model from type Ia supernova data (SNe Ia), observational Hubble data (OHD), baryon acoustic oscillation data (BAO) and cosmic microwave background shift parameter data (CMB) and show that the model parameter space is consistent with the cosmological observations thus making this a viable model for dark energy to explain the current accelerated expansion of the universe. This paper is organised as follows. In Sec. 2 we review the Einstein Yang-Mills Higgs action coupled to gravity and the equations of motion in FRW background to study the dynamical system. Construction of autonomous system and dynamics of cosmology is studied in Sec. 3. In Sec. 4 we discuss the various observational data and the formalism for analyses of those data. In this section we also confront this Higgs dark energy model with the observational data and present the results of our data analysis. Eventually we conclude in Sec. 5

2 Einstein Yang-Mills Higgs action

In what follows we describe the Higgs dark energy in presence of gauge field in background of Einstein's gravitation. The Einstein Yang-Mills Higgs action is given by [36, 37],

$$S = \int d^4x \sqrt{-g} \left(\frac{M_{\text{Pl}}^2}{2} R - \frac{1}{4} F_a^{\mu\nu} F_{\mu\nu}^a - (D^\mu \Phi)^\dagger (D_\mu \Phi) - V(\Phi) + \mathcal{L}_r + \mathcal{L}_m \right), \quad (1)$$

where M_{Pl} is the reduced Planck mass given by $M_{\text{Pl}} = 1/\sqrt{8\pi G}$, g is the determinant of spacetime metric, Φ is the complex Higgs doublet invariant under $\text{SU}(2)$ gauge symmetry, \mathcal{L}_r is the lagrangian for radiation and \mathcal{L}_m is the matter lagrangian. Here $F_{\mu\nu}^a$ is the rank-2 tensor that represents the non-Abelian gauge field and is given by

$$F_{\mu\nu}^a = \partial_\mu A_\nu^a - \partial_\nu A_\mu^a + \beta \epsilon_{bc}^a A_\mu^b A_\nu^c, \quad (2)$$

where A_μ^a is the gauge field, β is the coupling of $\text{SU}(2)$ group and ϵ_{bc}^a is the rank 3 Levi-Civita symbol. D_μ is the gauge covariant derivative given by

$$D_\mu = \nabla_\mu - i\beta \frac{\sigma_a}{2} A_\mu^a, \quad (3)$$

where ∇_μ is the spacetime covariant derivative and σ_a are the Pauli matrices. The complex Higgs doublet and its potential are respectively given by,

$$\Phi = \begin{pmatrix} \phi_1 + i\chi_1 \\ \phi_2 + i\chi_2 \end{pmatrix}, \quad (4)$$

where $\phi_1, \phi_2, \chi_1, \chi_2$ are real scalar fields and

$$V(\Phi) = \frac{\lambda}{4} (\Phi^\dagger \Phi - v^2)^2, \quad (5)$$

where v is the vacuum expectation value (VEV) of Higgs field.

It is evident from the observations [7] that our universe is homogeneous and isotropic on large scales. Hence the background spacetime of the universe is described by the Friedmann Lemaître Robertson Walker (FLRW) metric and is given by in spherically symmetric coordinates,

$$ds^2 = -dt^2 + a^2(t) (dr^2 + r^2 d\Omega^2), \quad (6)$$

where t is the cosmological time, $a(t)$ is scale factor for expanding universe and $d\Omega^2 = d\theta^2 + \sin^2 \theta d\phi^2$. The energy momentum tensor for the action in Eq. 1 is given by,

$$\begin{aligned} T_{\mu\nu} = & -F_{\mu\eta}^a F_{\nu a}^\eta - (D_\mu \Phi)^\dagger (D_\nu \Phi) - (D_\nu \Phi)^\dagger (D_\mu \Phi) + 2 \frac{\partial}{\partial g^{\mu\nu}} (\mathcal{L}_m + \mathcal{L}_r) \\ & - g_{\mu\nu} \left[-\frac{1}{4} F_a^{\mu\nu} F_{\mu\nu}^a - (D^\mu \Phi)^\dagger (D_\mu \Phi) - V(\Phi) + \mathcal{L}_r + \mathcal{L}_m \right]. \end{aligned} \quad (7)$$

The Einstein tensor $G_{\mu\nu}$ is diagonal for FLRW background spacetime and hence the off diagonal terms of energy momentum tensor should vanish. This condition makes the gauge field become $A_\mu^a = \delta_\mu^a f(t)$ [36] where $f(t)$ is the only degree of freedom in the gauge sector as allowed from the FLRW spacetime of the universe, a is the gauge index and i is the spatial index. As discussed in [37], this condition is not sufficient to avoid the non-zero contribution to the momentum density arising from the interaction between the Yang-Mills field and the Higgs field. Hence another additional condition which is required to establish the isotropy in energy momentum tensor is to fix the gauge so that

$$\Phi(t) = \begin{pmatrix} \phi(t) \\ 0 \end{pmatrix}, \quad (8)$$

where $\phi(t)$ is a real scalar field. With these choices of gauge field and gauge fixation for the Higgs field, we obtain

$$H^2 = \frac{1}{3M_{\text{Pl}}^2} \left[\frac{3}{2} \frac{\dot{f}(t)^2}{a(t)^2} + \dot{\phi}(t)^2 + \frac{3}{2} \frac{\beta^2 f(t)^4}{a(t)^4} + \frac{3}{4} \frac{\beta^2 \phi(t)^2 f(t)^2}{a(t)^2} + V(\phi) + \rho_m + \rho_r \right], \quad (9)$$

$$\dot{H} = -\frac{1}{2M_{\text{Pl}}^2} \left[2 \frac{\dot{f}(t)^2}{a(t)^2} + 2 \dot{\phi}(t)^2 + 2 \frac{\beta^2 f(t)^4}{a(t)^4} + \frac{\beta^2 \phi(t)^2 f(t)^2}{2a(t)^2} + \rho_m + \frac{4}{3} \rho_r \right], \quad (10)$$

where H is Hubble parameter given by $H = \dot{a}(t)/a(t)$ and ρ_m, ρ_r are the matter and radiation density respectively. The equation of motions of the gauge and Higgs fields are respectively given by,

$$\ddot{f}(t) + H\dot{f}(t) + \beta^2 \left[2\frac{f(t)^3}{a(t)^2} + \frac{f(t)\phi(t)^2}{2} \right] = 0, \quad (11)$$

$$\ddot{\phi}(t) + 3H\dot{\phi}(t) + \frac{3\beta^2 f(t)^2 \phi(t)}{4a(t)^2} + \frac{dV(\phi)}{d\phi} = 0, \quad (12)$$

where $V(\phi)$ is given by $V(\phi) = \frac{\lambda}{4}(\phi^2 - v^2)$. This is worth mentioning here that from Eq. (11) it is evident that there arises an effective potential for the gauge field with vanishing vacuum expectation value due to the interaction between the gauge field and the Higgs field. Moreover the same interaction leads to the effective potential of the Higgs field also as shown in the Eq. (12).

3 Dynamics of cosmology

To analyse the cosmological dynamics the following dimensionless variables are introduced here.

$$\begin{aligned} x_1 &= \frac{\dot{f}}{\sqrt{2}aM_{\text{Pl}}H}, & y_1 &= \frac{\beta f^2}{\sqrt{2}a^2M_{\text{Pl}}H}, \\ z_1 &= \frac{\beta f\phi}{2aM_{\text{Pl}}H}, & x_2 &= \frac{\dot{\phi}}{\sqrt{3}M_{\text{Pl}}H}, \\ y_2 &= \sqrt{\frac{V(\phi)}{3M_{\text{Pl}}^2H^2}}, & r &= \sqrt{\frac{\rho_r}{3M_{\text{Pl}}^2H^2}}, \\ m &= \sqrt{\frac{\rho_m}{3M_{\text{Pl}}^2H^2}}, & w_1 &= \frac{\sqrt{2}aM_{\text{Pl}}}{f}, \end{aligned} \quad (13)$$

The subscripts 1 and 2 refers to the dimensionless variables corresponding to gauge field and the Higgs field. With these choices the total energy density in the universe takes the form (from Eq. (9)),

$$x_1^2 + y_1^2 + z_1^2 + x_2^2 + y_2^2 + r^2 + m^2 = 1. \quad (14)$$

The evolution equations of the autonomous system are given by

$$\begin{aligned}
x'_1 &= x_1(q-1) - w_1(2y_1^2 + z_1^2), \\
y'_1 &= y_1(2x_1w_1 + q-1), \\
z'_1 &= z_1(x_1w_1 + q) + \frac{\sqrt{3}}{2}w_1y_1x_2, \\
x'_2 &= x_2(q-2) - z_1w_1(2\alpha y_2 + \frac{\sqrt{3}}{2}y_1), \\
y'_2 &= y_2(q+1) + \alpha w_1z_1x_2, \\
r' &= r(q-1), \\
m' &= m\left(q - \frac{1}{2}\right), \\
w'_1 &= w_1(1 - w_1x_1),
\end{aligned} \tag{15}$$

where the symbol prime denotes a derivative with respect to $N = \ln a$, a being the scale factor of the universe and q is the deceleration parameter defined as $q(t) = -\frac{\ddot{a}(t)a(t)}{\dot{a}(t)^2}$. In terms of the dimensionless variables defined above the deceleration parameter takes the form

$$q = \frac{1}{2}(1 + x_1^2 + y_1^2 - z_1^2 + 3x_2^2 - 3y_2^2 + r^2). \tag{16}$$

Here α is a dimensionless constant given by $\alpha = \sqrt{\frac{\lambda}{2\beta^2}}$.

We solve the autonomous system for the initial conditions given by $x_1 = 10^{-18}$, $y_1 = 10^{-18}$, $z_1 = 10^{-18}$, $x_2 = 10^{-18}$, $y_2 = 0.831$, $w_1 = 10^2$ and $r = 10^{-2}$ at $z = 0$ [36, 37]. In the Fig. 2, we show the variation of density of radiation, matter and dark energy with the number of e-foldings N and variation of the density parameters are shown in Fig. 1 for $\Omega_m^{(0)} = 0.31$ and $H_0 = 69 \text{ Kmsec}^{-1}\text{Mpc}^{-1}$ and $\alpha = 1$. From these two figures this is evident that the dark energy dominates very recently. Moreover it is evident from Fig. 2 that the Higgs dark energy though varies initially but starts mimicking the cosmological constant around $N = -12$ i.e., well in the radiation dominated era. The plot of the deceleration parameter q and the effective equation of state ω_{eff} of the universe for all the components i.e., radiation, matter and the dark energy are shown in Fig. 3. The acceleration of the universe corresponds to $q < 0$ and $\omega_{\text{eff}} < -1/3$.

4 Observational Constraints

In this era of precision cosmology models of dark energy are highly constrained. Passing the test of observational data only makes the model acceptable despite their theoretical viability. In this section we describe the observational data that are used to constrain the model parameter in this Einstein Yang-Mills Higgs dark energy and the formalism for the data analysis as well.

Supernovae Type Ia are accepted as the standard candles in astrophysical observations. Incidentally it happened to be the first probe for the discovery of the late time cosmic acceleration [1, 2]. We consider here 279 Supernovae Type Ia (SNe Ia) observational data

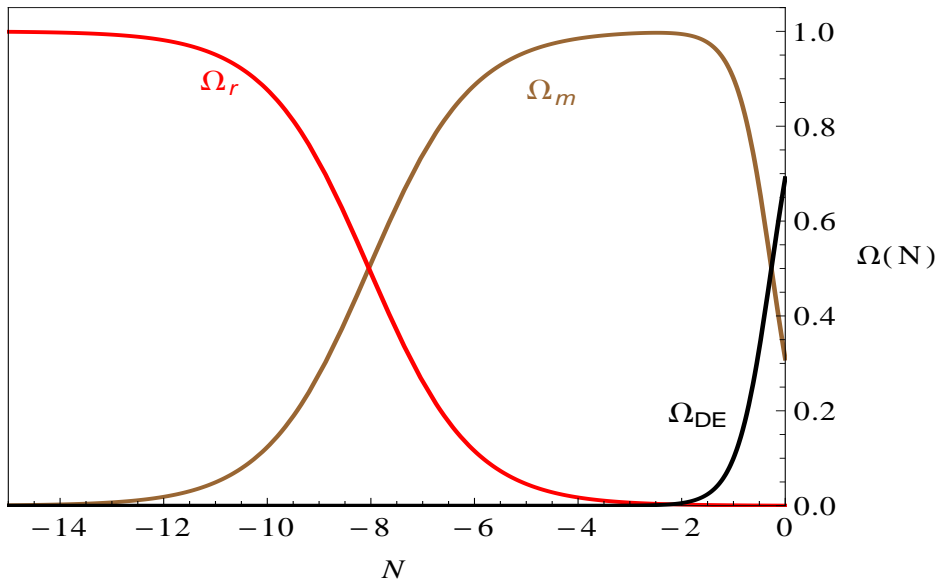


Figure 1: Plot of the density parameters in the Universe with the number of e-foldings N given by $N = -\ln(1+z)$ where z is the corresponding redshift.

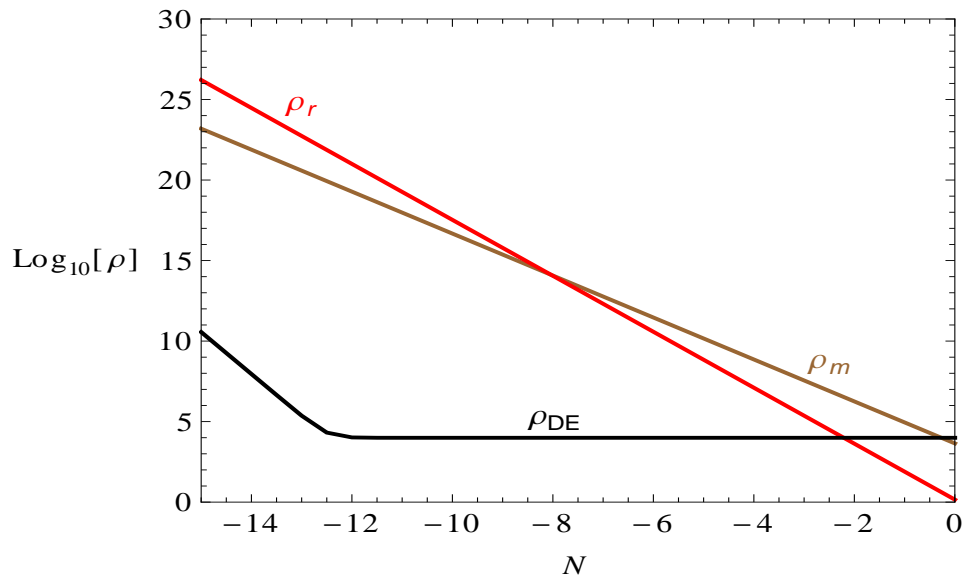


Figure 2: Plot of the density in the Universe number of e-foldings N given by $N = -\ln(1+z)$ where z is the corresponding redshift.

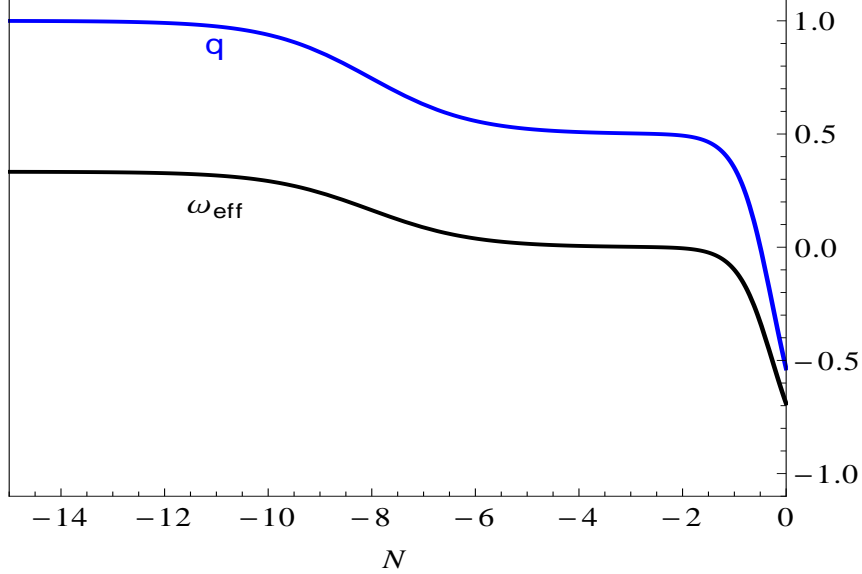


Figure 3: Plot of deceleration parameter q and effective equation of state of the universe ω_{eff} with the number of e-foldings N given by $N = -\ln(1+z)$ where z is the corresponding redshift.

from Pan-STARRS1 Medium Deep Survey in the redshift range $0.03 < z < 0.68$ along with the other SNe Ia data from Sloan Digital Sky Survey (SDSS) [38–40], SNLS [41, 42], and ESSENCE [43–45] and SCP [46]. The combined data set known as Pantheon Sample [47] consists of 1048 SNe Ia data points in the redshift range $0.01 < z < 2.3$. The distance modulus for type Ia supernova as a function of the redshift is given by

$$\mu(z) = 5 \log_{10}(D_L(z)) + \mu_0, \quad (17)$$

where $D_L(z) = H_0 d_L(z)/c$ (c is speed of light in free space) and $\mu_0 = 42.38 - 5 \log_{10} h$ for $H_0 = 100h \text{ Km Sec}^{-1} \text{ Mpc}^{-1}$. The chi-square for supernovae data is defined as

$$\chi_{\text{SN}}^2(p_s) = \sum_i \left[\frac{\mu_{\text{obs}}(z_i) - \mu_{\text{th}}(z_i, p_s, \mu_0)}{\sigma_i} \right]^2, \quad (18)$$

where p_s are the model parameters and z_i are the redshifts of the observational supernovae type Ia data. μ_{obs} and μ_{th} are the observational and theoretical distance modulus respectively. The chi-square is marginalised over the nuisance parameter μ_0 [48] and the marginalised chi-square is given by

$$\chi_{\text{SN}}^2 = A(p_s) - \frac{B(p_s)^2}{C}, \quad (19)$$

where A , B and C are given by

$$A(p_s) = \sum_i \left[\frac{\mu_{\text{obs}}(z_i) - \mu_{\text{th}}(z_i, p_s, \mu_0)}{\sigma_i} \right]^2, \quad (20)$$

$$B(p_s) = \sum_i \frac{\mu_{\text{obs}}(z_i) - \mu_{\text{th}}(z_i, p_s, \mu_0)}{\sigma_i^2}, \quad (21)$$

$$C = \sum_i \frac{1}{\sigma_i^2}, \quad (22)$$

Cosmic microwave background shift parameter R is a model independent parameter that can also be used to constrain the models of dark energy. It is obtained from the first peak of temperature anisotropy plot of the cosmic microwave background radiation. The CMBR shift parameter is defined as

$$R(z_*) = (\Omega_m^0 H_0^2)^{1/2} \int_0^{z_*} \frac{dz}{H(z)}, \quad (23)$$

where z_* corresponds to the redshift of the radiation matter decoupling epoch. The chi-square for CMBR shift parameter is defined as

$$\chi_{\text{CMB}}^2 = \left[\frac{R_{\text{th}}(z_*, p_s) - R_{\text{obs}}(z_*)}{\sigma_R} \right]^2. \quad (24)$$

Needless to mention that p_s are the model parameters. We use the CMBR shift parameter from latest Planck observations $R = 1.7499 \pm 0.0088$ at the redshift of decoupling era $z_* = 1091.41$ [49].

Observational Hubble data is a direct measurement of expansion rate of universe with the redshifts. It is another tool to constrain the dark energy models. The chi-square for observational Hubble data is given by

$$\chi_{\text{OHD}}^2 = \sum_i \left[\frac{H_{\text{obs}}(z_i) - H_{\text{th}}(z_i, p_s)}{\sigma_i^2} \right]^2, \quad (25)$$

We use the 31 data points of $H(z)$ for the purpose of χ_{OHD}^2 analysis. The measurements of observational Hubble data are summarized in Tab. 1 [57].

Before the recombination epoch the baryons were tightly coupled to the photons and as a result of this tight coupling the acoustic oscillations created small density fluctuations in baryon photon plasma. In the expanding universe, this density fluctuations left an imprint in the large scale structures which provides a standard ruler in cosmology. Baryon acoustic oscillation is the powerful tool for constraining dark energy models. The sound horizon at a redshift z_d for drag epoch is given by

$$r_d = \frac{c}{\sqrt{3}} \int_{z_d}^{\infty} \frac{dz}{\sqrt{1 + \frac{3\Omega_b^{(0)}}{4\Omega_{\gamma}^{(0)}} \frac{1}{1+z} H(z)}}, \quad (26)$$

z	$H(z)$ KmSec $^{-1}$ Mpc $^{-1}$	$\sigma_{H(z)}$ KmSec $^{-1}$ Mpc $^{-1}$
0.07	69.0	19.6 [50]
0.09	69.0	12.0 [51]
0.12	68.6	26.2 [50]
0.17	83.0	8.0 [51]
0.179	75.0	4.0 [52]
0.199	75.0	5.0 [52]
0.2	72.9	29.6 [50]
0.27	77.0	14.0 [51]
0.28	88.8	36.6 [50]
0.352	83.0	14.0 [52]
0.3802	83.0	13.5 [53]
0.4	95.0	17.0 [51]
0.4004	77.0	10.2 [53]
0.4247	87.1	11.2 [53]
0.4497	92.8	12.9 [53]
0.47	89.0	49.6 [54]
0.4783	80.9	9.0 [53]
0.48	97.0	62.0 [55]
0.593	104.0	13.0 [52]
0.68	92.0	8.0 [52]
0.781	105.0	12.0 [52]
0.875	125.0	17.0 [52]
0.88	90.0	40.0 [55]
0.9	117.0	23.0 [51]
1.037	154.0	20.0 [52]
1.3	168.0	17.0 [51]
1.363	160.0	33.6 [56]
1.43	177.0	18.0 [51]
1.53	140.0	14.0 [51]
1.75	202.0	40.0 [51]
1.965	186.5	50.4 [56]

Table 1: The 31 $H(z)$ data points [57].

Data set	Redshift	$D_V(z)/r_d$
6dF	z=0.106	2.98 ± 0.13 [59]
MGS	z=0.15	4.47 ± 0.17 [60]
eBOSS quasars	z=1.52	26.1 ± 1.1 [61]

Table 2: Isotropic BAO data.

Data set	Redshift	$D_{A/H}(z)/r_d$
BOSS DR12	z=0.38	$7.42(A)$ [62]
BOSS DR12	z=0.38	$24.97(H)$ [62]
BOSS DR12	z=0.51	$8.85(A)$ [62]
BOSS DR12	z=0.51	$22.31(H)$ [62]
BOSS DR12	z=0.61	$9.69(A)$ [62]
BOSS DR12	z=0.61	$20.49(H)$ [62]
BOSS DR12	z=2.4	$10.76(A)$ [63]
BOSS DR12	z=2.4	$8.94(H)$ [63]

Table 3: Anisotropic BAO data.

where the drag redshift z_d is given by

$$z_d = \frac{1291 \left(\Omega_m^{(0)} h^2 \right)^{0.251}}{1 + 0.659 \left(\Omega_m^{(0)} h^2 \right)^{0.828}} \left[1 + b_1 \left(\Omega_b^{(0)} h^2 \right)^{b_2} \right], \quad (27)$$

with

$$b_1 = 0.313 \left(\Omega_b^{(0)} h^2 \right)^{-0.419} \left[1 + 0.607 \left(\Omega_m^{(0)} h^2 \right)^{0.674} \right], \quad (28)$$

$$b_2 = 0.238 \left(\Omega_m^{(0)} h^2 \right)^{0.223}, \quad (29)$$

and $\Omega_b^{(0)} h^2 = 0.02236$, $\Omega_\gamma^{(0)} h^2 = 2.469 \times 10^{-5}$ [7]. In a spatially flat universe the angular diameter distance $D_A(z)$, the Hubble distance $D_H(z)$ and the effective distance $D_V(z)$ are respectively given by,

$$D_A(z) = \frac{c}{(1+z)} \int_0^z \frac{dz}{H(z)}, \quad (30)$$

$$D_H(z) = \frac{c}{H(z)}, \quad (31)$$

$$D_V(z) = \left[\left(\frac{d_L(z)}{1+z} \right)^2 \frac{cz}{H(z)} \right]^{1/3} \quad (32)$$

where c the speed of light in vacuum. Here we use both the isotropic and anisotropic BAO data that are tabulated in Tabs. 2 and 3 [58]. The covariance matrix \mathbf{C} associated with

the anisotropic BAO measurements is given by

$$\mathbf{C} = \begin{pmatrix} 0.0150 & -0.0357 & 0.0071 & -0.0100 & 0.0032 & -0.0036 & 0 & 0 \\ -0.0357 & 0.5304 & -0.0160 & 0.1766 & -0.0083 & 0.0616 & 0 & 0 \\ 0.0071 & -0.0160 & 0.0182 & -0.0323 & 0.0097 & -0.0131 & 0 & 0 \\ -0.0100 & 0.1766 & -0.0323 & 0.3267 & -0.0167 & 0.1450 & 0 & 0 \\ 0.0032 & -0.0083 & 0.0097 & -0.0167 & 0.0243 & -0.0352 & 0 & 0 \\ -0.0036 & 0.0616 & -0.0131 & 0.1450 & -0.0352 & 0.2684 & 0 & 0 \\ 0 & 0 & 0 & 0 & 0 & 0 & 0.1358 & -0.0296 \\ 0 & 0 & 0 & 0 & 0 & 0 & -0.0296 & 0.0492 \end{pmatrix}.$$

The total chi-square for isotropic and anisotropic BAO data is given by

$$\chi_{\text{BAO}}^2 = \chi_{\text{iso}}^2 + \chi_{\text{aniso}}^2, \quad (33)$$

where

$$\chi_{\text{iso}}^2 = \sum_i \left[\frac{D_V(z_i)/r_d - D_V(z_i, p_s)/r_d}{\sigma_i} \right]^2, \quad (34)$$

$$\chi_{\text{aniso}}^2 = \mathbf{X}_{\text{aniso}}^T \mathbf{C}^{-1} \mathbf{X}_{\text{aniso}} \quad (35)$$

where $\mathbf{X}_{\text{aniso}}$ is column matrix given by,

$$\mathbf{X}_{\text{aniso}} = \begin{pmatrix} \frac{D_A(0.38)}{r_d} - 7.42 \\ \frac{D_H(0.38)}{r_d} - 24.97 \\ \frac{D_A(0.51)}{r_d} - 8.85 \\ \frac{D_H(0.51)}{r_d} - 22.31 \\ \frac{D_A(0.61)}{r_d} - 9.69 \\ \frac{D_H(0.61)}{r_d} - 20.49 \\ \frac{D_A(2.4)}{r_d} - 10.76 \\ \frac{D_H(2.4)}{r_d} - 8.94 \end{pmatrix}. \quad (36)$$

The total combined chi-square for all the aforesaid data sets i.e., SNe Ia, CMB shift parameter, OHD, BAO is given by,

$$\chi_{\text{tot}}^2 = \chi_{\text{SN}}^2 + \chi_{\text{OHD}}^2 + \chi_{\text{BAO}}^2 + \chi_{\text{CMB}}^2. \quad (37)$$

We use this total chisquare defined in Eq. (37) for the data analysis purpose of the Yang-Mills Higgs dark energy model and constrain the parameters space.

In what follows, we describe the model parameters and the results of the chi-square analysis of the observational data. In this Higgs dark energy model we consider four parameters namely α , $\Omega_m^{(0)}$, H_0 and $H_0 r_d/c$ to fit the chi-square with the latest observational data from SNe Ia, OHD, BAO and CMB. In the Fig. 4, we present the 68.3%, 90% and 99% confidence level plot for the parameters $\Omega_m^{(0)}$ and H_0 with the contour shadding by the light blue, dark blue and cyan colours respectively. The total chi-square turns out to have a minima at

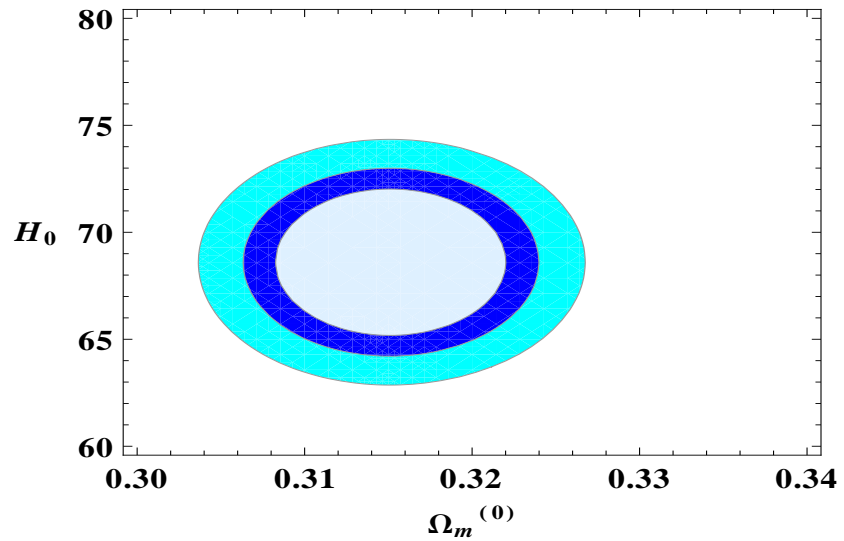


Figure 4: Observational constraints on the parameters space $(\Omega_m^{(0)} - H_0)$ at the 68.3% (light blue), 90% (dark blue) and 99% (cyan) confidence levels.

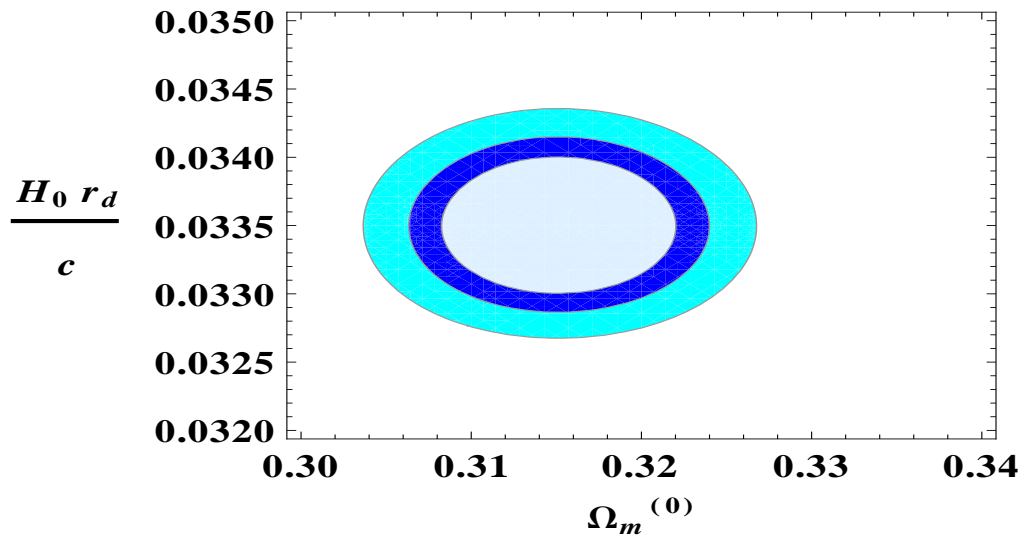


Figure 5: Observational constraints on the parameters space $(\Omega_m^{(0)} - H_0 r_d / c)$ at the 68.3% (light blue), 90% (dark blue) and 99% (cyan) confidence levels.

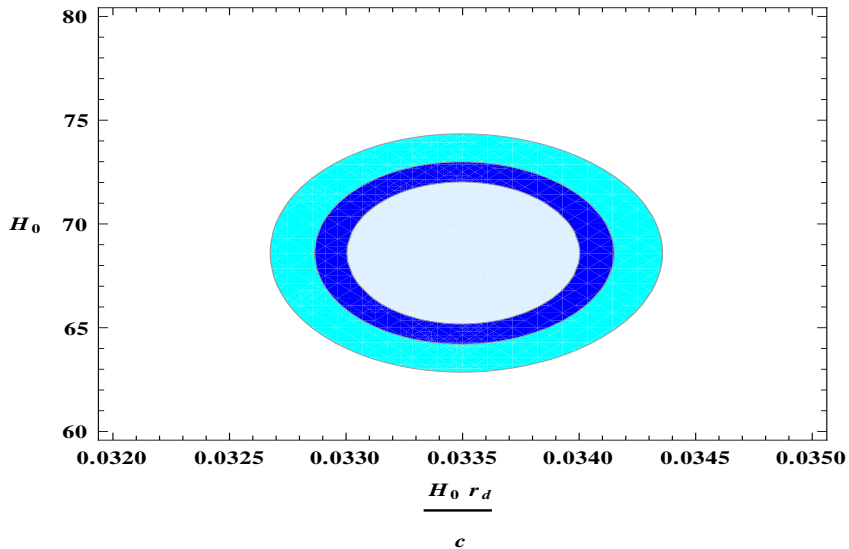


Figure 6: Observational constraints on the parameters space ($H_0 r_d/c - H_0$) at the 68.3% (light blue), 90% (dark blue) and 99% (cyan) confidence levels.

$\Omega_m^{(0)} \simeq 0.315$ and $H_0 \simeq 68.6 \text{ KmSec}^{-1}\text{Mpc}^{-1}$ and $H_0 r_d/c \simeq 0.0335$ which with the best-fit value of H_0 and speed of light in vacuum gives $r_d \simeq 146.5$ Mpc. Fig. 5 and 6 shows the observationally allowed parameters space in $\Omega_m^{(0)} - H_0 r_d/c$ and $H_0 r_d/c - H_0$ at 68.3%, 90% and 99% confidence levels with the same colours mentioned above. It is worth mentioning here that all this confidence contours corresponds to value of $\alpha = 1$ [64]. The parameter α cannot be constrained from the present observational data we have considered here. A confidence contour is shown in Fig. 7 in the $\alpha - \Omega_m^{(0)}$ parameters space from where it is evident that the present data is unable to put any bound on the parameter α . With a total of 1091 data points from SNe Ia, OHD, BAO and CMB, we find from our data analysis a chi-square per degrees of freedom to be around 0.983 i.e., very close to 1 which in turn reflects the fact that the fitment of the model parameters are in good agreement with the observational data sets [65].

5 Conclusion

In this work, we study Higgs dark energy model in presence of gauge field in light of observational data from supernovae type Ia, baryon acoustic oscillation, observational Hubble data and cosmic microwave background shift parameter data. In performing the data analysis, we considered the initial conditions at the present epoch for dynamical evolution of the autonomous system. The choice of initial condition for Higgs field is in consideration with the vacuum expectation value of Higgs $v \sim 246$ GeV that leads to initial values of $x_1 = 10^{-18}$, $y_1 = 10^{-18}$, $z_1 = 10^{-18}$, $x_2 = 10^{-18}$, $y_2 = 0.831$, $w_1 = 10^2$ and $r = 10^{-2}$ at $z = 0$ i.e., present epoch [36, 37]. These choice of initial conditions lead to correct cosmological dynamics for the observational universe as evident from Fig 2 and the cosmic acceleration is a recent phenomenon. Moreover from the same figure it appears that the Higgs dark

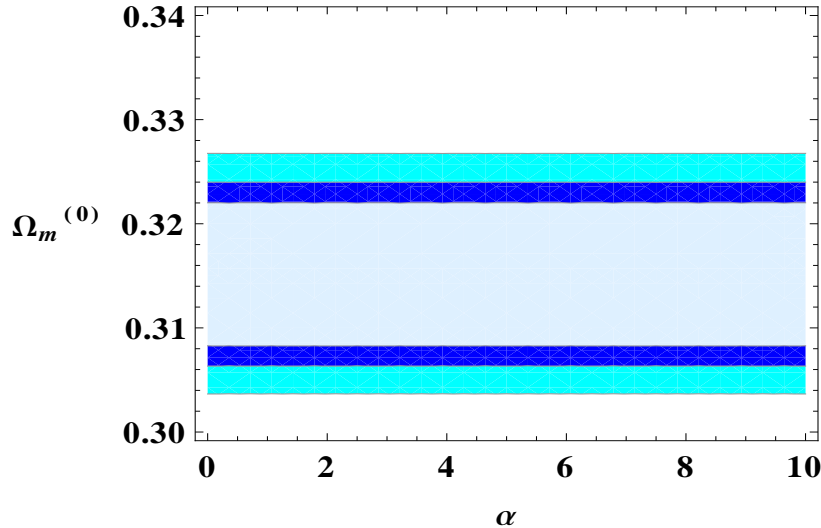


Figure 7: Observational constraints on the parameters space $(\alpha - \Omega_m^{(0)})$ at the 68.3% (light blue), 90% (dark blue) and 99% (cyan) confidence levels.

energy starts mimicking cosmological constant well in the radiation dominated era. The chi-square analysis of the observational data significantly constrains the model parameters $(\alpha, \Omega_m^{(0)}, H_0, H_0 r_d/c)$. The minimum combined chi-square for all the data sets is obtained at the parameter values $(\Omega_m^{(0)}, H_0, H_0 r_d/c) \sim (0.315, 68.6, 0.0335)$. Hence the sound horizon at the redshift of drag epoch turns out to be around 146.5 Mpc which is in remarkably good agreement with the Planck 2018 results [7]. Also this is worth mentioning here that the chi-square per degrees of freedom is slightly greater than 0.98 which is the indication of a good fitting of the model with the observational data [65]. However data is still unable to provide any constraint on the model parameter α as is evident from Fig. 7. Needless to mention that the Higgs or the gauge field in the theory being minimally coupled to gravity does not conflict with the observational evidences of gravitational wave detection [17, 18, 21]. Thus the Higgs field in presence of gauge field turns out to be a viable candidate for dark energy so far as the observational data are concerned.

References

- [1] Adam G. Riess et al. Observational evidence from supernovae for an accelerating universe and a cosmological constant. *Astron.J.*, 116:1009–1038, 1998.
- [2] S. Perlmutter et al. Measurements of Omega and Lambda from 42 high redshift supernovae. *Astrophys.J.*, 517:565–586, 1999.
- [3] Robert R. Caldwell and Marc Kamionkowski. The Physics of Cosmic Acceleration. *Ann. Rev. Nucl. Part. Sci.*, 59:397–429, 2009.

- [4] Joshua Frieman, Michael Turner, and Dragan Huterer. Dark Energy and the Accelerating Universe. *Ann. Rev. Astron. Astrophys.*, 46:385–432, 2008.
- [5] P. J. E. Peebles and Bharat Ratra. The cosmological constant and dark energy. *Rev. Mod. Phys.*, 75:559–606, Apr 2003.
- [6] Eric V Linder. Mapping the cosmological expansion. *Reports on Progress in Physics*, 71(5):056901, apr 2008.
- [7] N. Aghanim et al. Planck 2018 results. VI. Cosmological parameters. 7 2018.
- [8] L. Amendola and S. Tsujikawa. *Dark Energy: Theory and Observations*. Cambridge University Press, 2010.
- [9] R. R. Caldwell, Rahul Dave, and Paul J. Steinhardt. Cosmological imprint of an energy component with general equation of state. *Phys. Rev. Lett.*, 80:1582–1585, Feb 1998.
- [10] Paul J. Steinhardt, Limin Wang, and Ivaylo Zlatev. Cosmological tracking solutions. *Phys. Rev. D*, 59:123504, May 1999.
- [11] Salvatore Capozziello. Curvature quintessence. *Int. J. Mod. Phys. D*, 11:483–492, 2002.
- [12] Salvatore Capozziello, Sante Carloni, and Antonio Troisi. Quintessence without scalar fields. *Recent Res. Dev. Astron. Astrophys.*, 1:625, 2003.
- [13] S. Capozziello, V.F. Cardone, S. Carloni, and A. Troisi. Curvature quintessence matched with observational data. *Int. J. Mod. Phys. D*, 12:1969–1982, 2003.
- [14] Alberto Nicolis, Riccardo Rattazzi, and Enrico Trincherini. The Galileon as a local modification of gravity. *Phys. Rev.*, D79:064036, 2009.
- [15] Antonio De Felice and Shinji Tsujikawa. Cosmology of a covariant Galileon field. *Phys. Rev. Lett.*, 105:111301, 2010.
- [16] Timothy Clifton, Pedro G. Ferreira, Antonio Padilla, and Constantinos Skordis. Modified Gravity and Cosmology. *Phys. Rept.*, 513:1–189, 2012.
- [17] B. P. Abbott et. al.. Gw170817: Observation of gravitational waves from a binary neutron star inspiral. *Phys. Rev. Lett.*, 119:161101, Oct 2017.
- [18] A. Goldstein et. al.. An ordinary short gamma-ray burst with extraordinary implications: Fermi -GBM detection of GRB 170817a. *The Astrophysical Journal*, 848(2):L14, oct 2017.
- [19] V. Savchenko et. al.. INTEGRAL detection of the first prompt gamma-ray signal coincident with the gravitational-wave event GW170817. *The Astrophysical Journal*, 848(2):L15, oct 2017.
- [20] B. P. Abbott et. al.. Multi-messenger observations of a binary neutron star merger. *The Astrophysical Journal*, 848(2):L12, oct 2017.

- [21] B. P. Abbott et. al.. Gravitational waves and gamma-rays from a binary neutron star merger: GW170817 and GRB 170817a. *The Astrophysical Journal*, 848(2):L13, oct 2017.
- [22] T. Baker, E. Bellini, P. G. Ferreira, M. Lagos, J. Noller, and I. Sawicki. Strong constraints on cosmological gravity from gw170817 and grb 170817a. *Phys. Rev. Lett.*, 119:251301, Dec 2017.
- [23] Paolo Creminelli and Filippo Vernizzi. Dark energy after gw170817 and grb170817a. *Phys. Rev. Lett.*, 119:251302, Dec 2017.
- [24] Jeremy Sakstein and Bhuvnesh Jain. Implications of the neutron star merger gw170817 for cosmological scalar-tensor theories. *Phys. Rev. Lett.*, 119:251303, Dec 2017.
- [25] Jose María Ezquiaga and Miguel Zumalacárregui. Dark energy after gw170817: Dead ends and the road ahead. *Phys. Rev. Lett.*, 119:251304, Dec 2017.
- [26] Paolo Creminelli, Matthew Lewandowski, Giovanni Tambalo, and Filippo Vernizzi. Gravitational wave decay into dark energy. *Journal of Cosmology and Astroparticle Physics*, 2018(12):025–025, dec 2018.
- [27] Paolo Creminelli, Giovanni Tambalo, Filippo Vernizzi, and Vicharit Yingcharoenrat. Resonant decay of gravitational waves into dark energy. *Journal of Cosmology and Astroparticle Physics*, 2019(10):072–072, oct 2019.
- [28] Johannes Noller. Cosmological constraints on dark energy in light of gravitational wave bounds. *Phys. Rev. D*, 101(6):063524, 2020.
- [29] Steven Weinberg. *The Quantum Theory of Fields*, volume 2. Cambridge University Press, 1996.
- [30] A. Das. *Lectures on Quantum Field Theory*. World Scientific, 2008.
- [31] M. Henneaux. REMARKS ON SPACE-TIME SYMMETRIES AND NONABELIAN GAUGE FIELDS. *J. Math. Phys.*, 23:830–833, 1982.
- [32] D.V. Galt'sov and M.S. Volkov. Yang-mills cosmology. cold matter for a hot universe. *Physics Letters B*, 256(1):17 – 21, 1991.
- [33] P.V. Moniz and J.M. Mourao. Homogeneous and isotropic closed cosmologies with a gauge sector. *Class. Quant. Grav.*, 8:1815–1832, 1991.
- [34] P V Moniz, J M Mourao, and P M Sa. The dynamics of a flat friedmann-robertson-walker inflationary model in the presence of gauge fields. *Classical and Quantum Gravity*, 10(3):517–534, mar 1993.
- [35] U. Ochs and M. Sorg. Cosmological solutions for the coupled Einstein-Yang-Mills-Higgs equations. *Gen. Rel. Grav.*, 28:1177–1219, 1996.
- [36] Massimiliano Rinaldi. Higgs Dark Energy. *Class. Quant. Grav.*, 32:045002, 2015.

[37] Miguel Álvarez, J. Bayron Orjuela-Quintana, Yeinzon Rodriguez, and Cesar A. Valenzuela-Toledo. Einstein Yang–Mills Higgs dark energy revisited. *Class. Quant. Grav.*, 36(19):195004, 2019.

[38] Joshua A. Frieman and et. al.. THE SLOAN DIGITAL SKY SURVEY-II SUPERNOVA SURVEY: TECHNICAL SUMMARY. *The Astronomical Journal*, 135(1):338–347, dec 2007.

[39] Richard Kessler and et. al.. FIRST-YEAR SLOAN DIGITAL SKY SURVEY-II SUPERNOVA RESULTS: HUBBLE DIAGRAM AND COSMOLOGICAL PARAMETERS. *The Astrophysical Journal Supplement Series*, 185(1):32–84, oct 2009.

[40] Masao Sako et al. The Data Release of the Sloan Digital Sky Survey-II Supernova Survey. *Publ. Astron. Soc. Pac.*, 130(988):064002, 2018.

[41] A. Conley et. al.. SUPERNOVA CONSTRAINTS AND SYSTEMATIC UNCERTAINTIES FROM THE FIRST THREE YEARS OF THE SUPERNOVA LEGACY SURVEY. *The Astrophysical Journal Supplement Series*, 192(1):1, dec 2010.

[42] M. Sullivan and et. al.. SNLS3: Constraints on Dark Energy Combining the Supernova Legacy Survey Three-year Data with Other Probes. *ApJ*, 737(2):102, August 2011.

[43] G. Miknaitis and et. al.. The ESSENCE supernova survey: Survey optimization, observations, and supernova photometry. *The Astrophysical Journal*, 666(2):674–693, sep 2007.

[44] W. M. Wood-Vasey and et. al.. Observational constraints on the nature of dark energy: First cosmological results from the ESSENCE supernova survey. *The Astrophysical Journal*, 666(2):694–715, sep 2007.

[45] G. Narayan and et. al.. LIGHT CURVES OF 213 TYPE ia SUPERNOVAE FROM THE ESSENCE SURVEY. *The Astrophysical Journal Supplement Series*, 224(1):3, may 2016.

[46] N. Suzuki, D. Rubin, C. Lidman, G. Aldering, R. Amanullah, et al. The Hubble Space Telescope Cluster Supernova Survey: V. Improving the Dark Energy Constraints Above $z > 1$ and Building an Early-Type-Hosted Supernova Sample. *Astrophys.J.*, 746:85, 2012.

[47] D. M. Scolnic, D. O. Jones, A. Rest, Y. C. Pan, R. Chornock, R. J. Foley, M. E. Huber, R. Kessler, G. Narayan, A. G. Riess, S. Rodney, E. Berger, D. J. Brout, P. J. Challis, M. Drout, D. Finkbeiner, R. Lunnan, R. P. Kirshner, N. E. Sanders, E. Schlafly, S. Smartt, C. W. Stubbs, J. Tonry, W. M. Wood-Vasey, M. Foley, J. Hand, E. Johnson, W. S. Burgett, K. C. Chambers, P. W. Draper, K. W. Hodapp, N. Kaiser, R. P. Kudritzki, E. A. Magnier, N. Metcalfe, F. Bresolin, E. Gall, R. Kotak, M. McCrum, and K. W. Smith. The Complete Light-curve Sample of Spectroscopically Confirmed SNe Ia from Pan-STARRS1 and Cosmological Constraints from the Combined Pantheon Sample. *ApJ*, 859(2):101, June 2018.

[48] R. Lazkoz, S. Nesseris, and Leandros Perivolaropoulos. Exploring Cosmological Expansion Parametrizations with the Gold SnIa Dataset. *JCAP*, 11:010, 2005.

[49] P.A.R. Ade et al. Planck 2013 results. XVI. Cosmological parameters. 2013.

[50] Cong Zhang, Han Zhang, Shuo Yuan, Siqi Liu, Tong-Jie Zhang, and Yan-Chun Sun. Four new observational $H(z)$ data from luminous red galaxies in the Sloan Digital Sky Survey data release seven. *Research in Astronomy and Astrophysics*, 14(10):1221–1233, October 2014.

[51] Joan Simon, Licia Verde, and Raul Jimenez. Constraints on the redshift dependence of the dark energy potential. *Phys. Rev. D*, 71:123001, 2005.

[52] M. Moresco et. al.. Improved constraints on the expansion rate of the Universe up to $z \sim 1.1$ from the spectroscopic evolution of cosmic chronometers. *Journal of Cosmology and Astroparticle Physics*, 2012(8):006, August 2012.

[53] Michele Moresco, Lucia Pozzetti, Andrea Cimatti, Raul Jimenez, Claudia Maraston, Licia Verde, Daniel Thomas, Annalisa Citro, Rita Tojeiro, and David Wilkinson. A 6% measurement of the Hubble parameter at $z \sim 0.45$: direct evidence of the epoch of cosmic re-acceleration. *JCAP*, 05:014, 2016.

[54] A.L. Ratsimbazafy, S.I. Loubser, S.M. Crawford, C.M. Cress, B.A. Bassett, R.C. Nichol, and P. Visnen. Age-dating Luminous Red Galaxies observed with the Southern African Large Telescope. *Mon. Not. Roy. Astron. Soc.*, 467(3):3239–3254, 2017.

[55] Daniel Stern, Raul Jimenez, Licia Verde, Marc Kamionkowski, and S. Adam Stanford. Cosmic chronometers: constraining the equation of state of dark energy. I: $H(z)$ measurements. *JCAP*, 2010(2):008, February 2010.

[56] Michele Moresco. Raising the bar: new constraints on the Hubble parameter with cosmic chronometers at $z \sim 2$. *Mon. Not. Roy. Astron. Soc.*, 450(1):L16–L20, 2015.

[57] Yingjie Yang and Yungui Gong. The evidence of cosmic acceleration and observational constraints. *JCAP*, 06:059, 2020.

[58] Jarah Evslin, Anjan A Sen, and Ruchika. Price of shifting the Hubble constant. *Phys. Rev. D*, 97(10):103511, 2018.

[59] Florian Beutler, Chris Blake, Matthew Colless, D. Heath Jones, Lister Staveley-Smith, et al. The 6dF Galaxy Survey: Baryon Acoustic Oscillations and the Local Hubble Constant. *Mon. Not. Roy. Astron. Soc.*, 416:3017–3032, 2011.

[60] Ashley J. Ross, Lado Samushia, Cullan Howlett, Will J. Percival, Angela Burden, and Marc Manera. The clustering of the SDSS DR7 main Galaxy sample – I. A 4 per cent distance measure at $z = 0.15$. *Mon. Not. Roy. Astron. Soc.*, 449(1):835–847, 2015.

[61] Metin Ata et al. The clustering of the SDSS-IV extended Baryon Oscillation Spectroscopic Survey DR14 quasar sample: first measurement of baryon acoustic oscillations between redshift 0.8 and 2.2. *Mon. Not. Roy. Astron. Soc.*, 473(4):4773–4794, 2018.

- [62] Shadab Alam et al. The clustering of galaxies in the completed SDSS-III Baryon Oscillation Spectroscopic Survey: cosmological analysis of the DR12 galaxy sample. *Mon. Not. Roy. Astron. Soc.*, 470(3):2617–2652, 2017.
- [63] Hlion du Mas des Bourboux et al. Baryon acoustic oscillations from the complete SDSS-III Ly α -quasar cross-correlation function at $z = 2.4$. *Astron. Astrophys.*, 608:A130, 2017.
- [64] J. Bayron Orjuela-Quintana, Miguel Alvarez, Cesar A. Valenzuela-Toledo, and Yeinzon Rodriguez. Anisotropic Einstein Yang-Mills Higgs Dark Energy. 6 2020.
- [65] Philip R Bevington and D Keith Robinson. *Data reduction and error analysis for the physical sciences; 3rd ed.* McGraw-Hill, New York, NY, 2003.